Synthesis, Characterization, and Aqueous Self-Assembly of Amphiphilic Poly(ethylene oxide)-Functionalized Hyperbranched Fluoropolymers

WENJUN DU, YALI LI, ANDREAS M. NYSTRÖM,* CHONG CHENG,† KAREN L. WOOLEY‡

Departments of Chemistry and Radiology, Washington University in Saint Louis, Saint Louis, Missouri 63130

Received 3 June 2009; accepted 22 May 2010
DOI: 10.1002/pola.24149
Published online in Wiley InterScience (www.interscience.wiley.com).

ABSTRACT: Complex amphiphilic polymers were synthesized via core-first polymerization followed by alkylation-based grafting of poly(ethylene oxide) (PEO). Inimer 1-(4′-(bromomethyl)-benzyloxy)-2,3,5,6-tetrafluoro-4-vinylbenzene was synthesized and subjected to atom transfer radical self-condensing vinyl polymerization to afford hyperbranched fluoropolymer (HBFP) as the hydrophobic core component with a number-averaged molecular weight of 29 kDa and polydispersity index of 2.1. The alkyl halide chain ends on the HBFP were allowed to undergo reaction with monomethoxy-terminated poly(ethylene oxide) amine (PEO_x-NH_2) at different grafting numbers and PEO chain lengths to afford PEO-functionalized HBFPs [$(PEO_x)_y$-HBFPs], with $x = 15$ while $y = 16$, 22, or 29, $x = 44$ while $y = 16$, and $x = 112$ while $y = 16$. The amphiphilic, grafted block copolymers were found to aggregate in aqueous solution to give micelles with number-averaged diameters (D_{av}) of 12–28 nm, as measured by transmission electron microscopy (TEM). An increase of the PEO:HBFP ratio, by increase in either the grafting densities (y values) or the chain lengths (x values), led to decreased TEM-measured diameters. These complex, amphiphilic $(PEO_x)_y$-HBFPs, with tunable sizes, might find potential applications as nanoscopic biomedical devices, such as drug delivery vehicles and ^{19}F magnetic resonance imaging agents. © 2010 Wiley Periodicals, Inc. J Polym Sci Part A: Polym Chem 48: 3487–3496, 2010

KEYWORDS: amphiphiles; fluoropolymers; hyperbranched; micelles; self-assembly

INTRODUCTION The self-assembly of amphiphilic polymers to construct various unique macromolecular morphologies and to define three-dimensional complexities into nanostructured materials in the bulk or solution states has drawn increasing attention because of their promise toward applications in the fields of advanced technologies, such as in the electronics industry[1–7] and biomedical research, including gene therapy and drug delivery.[8–14] Discrete nanoscale objects result from assembly of amphiphilic block copolymers of various architectures, in dilute solution, for which many architectures have been observed, for example, toroids,[15] helices,[16] rods,[17] disks,[18,19] and multicompartment micelles (MCMs).[20–26] Among them, MCMs are of special interest because these materials have shown the potential to uptake two or more compounds with different structures or properties, such as genes, therapeutics, and imaging agents, and to concurrently transport and deliver them to the target in a prescribed manner, thus creating the promise of a novel delivery approach called "double delivery" or "smart delivery."[27–31] For example, Lodge et al. have demonstrated that amphiphilic MCMs composed of poly(ethylene oxide) (PEO), polyethylethylene (PEE), and poly(perfluoropropylene oxide) (PFPO) were able to encapsulate two distinct and immiscible dyes, pyrene and 1-naphthyl perfluoroheptanyl ketone simultaneously, without interfering with one another.[27] This model study for the "double delivery" approach could be useful, especially with certain disease states, for which more than one drug is administered in a controlled manner. The unique uptake and release potential of MCMs may provide a practical device for such applications.

To produce MCMs, multiblock polymers or miktoarm block polymers containing mutually immiscible block segments are usually required because AB diblock polymers often give core–shell micelles or vesicles. Upon self-assembly of unique polymer structures, together also with the possibility for variation in the solvent mixture and for the inclusion of additives,[32,33] the multiple irreconcilable components rearrange, whereby attraction of the like components and repulsion of the dissimilar segments drive reorganization and regrouping, which can afford several compartments or environments within one single micelle.[21,22,26,27]

Hyperbranched polymers can be conveniently synthesized from condensation of $A_x + B_y$[34] or AB_x monomers,[35] self-

Present address: Department of Neuroscience and The Swedish Medical Nanoscience Center, Karolinska Institute, SE-17776 Stockholm, Sweden.
†*Present address*: Department of Chemical and Biological Engineering, the State University of New York at Buffalo, Buffalo, New York 14260.
‡*Present address*: Department of Chemistry, Texas A&M University, College Station, Texas 77842.
Correspondence to: K. L. Wooley (E-mail: wooley@chem.tamu.edu)
Journal of Polymer Science: Part A: Polymer Chemistry, Vol. 48, 3487–3496 (2010) © 2010 Wiley Periodicals, Inc.

condensing vinyl polymerizations (SCVP),[36–41] and from radical polymerization techniques such as nitroxide-mediated polymerization[42] using mixtures of monofunctional and difunctional monomers. Upon further chemical modification or polymerization, amphiphilic polymers can be produced, which may exhibit unique self-assembly properties.[43–52] Because of the hyperbranched architecture of the polymers, complex micelles or MCMs are often produced.[44,45,47] For example, Mao et al. described the formation of MCMs from self-assembly of hyperbranched star copolymers having a poly(3-ethyl-3-hydroxymethyl)oxetane core, extended with the growth of 2-(*N,N*-dimethyl amino)ethyl methacrylate (DMAEMA) and 2,2,3,3,4,4,5,5-octafluoropentyl methacrylate (OFPMA) block copolymer arms. The MCMs were produced because of the hyperbranched architecture and the incompatibility of POFPMA with both the hyperbranched polyether and hydrophilic PDMAEMA segments.[44]

We are especially interested in the construction of MCMs from amphiphilic hyperbranched fluoropolymers (HBFPs) to serve as ^{19}F imaging and delivery agents.[14] Previously, it has been demonstrated that upon PEGylation of HBFPs, either to create amphiphilic macromolecules[43] or nanoscopically resolved crosslinked networks,[53–56] MCM-type nanostructures were produced, which exhibited unique properties such as promoted release of small guest molecules[54] and unusual mechanical properties.[55] Recently, we reported the syntheses of complex amphiphilic HBFPs via atom transfer radical self-condensing vinyl polymerization (ATR-SCVP) of a tri(ethylene glycol) (TEG)-functionalized tetrafluorostyrene inimer.[43] We have investigated the self-assemblies of these HBFPs in water and observed micellar structures having number-average hydrodynamic diameters $(D_h)_n$ of 170–190 nm.[43] The construction of micelles from such amphiphilic HBFPs prompted further exploration of the self-assembly behaviors of PEO-functionalized HBFPs to refine the sizes and architectures of the macromolecules and their micelles, and to investigate the possibility of creating MCMs with 20–30 nm sizes for *in vivo* imaging and delivery applications. Such MCMs were designed to package hydrophobic therapeutic agents and serve as ^{19}F-based MR imaging agents, as well. We hypothesized that if sufficient ethylene oxide (EO) units were anchored within the HBFP core, creating strong PEO shielding and allowing the EO units to extend into the aqueous environment to produce a pseudo-core–shell morphology, a decrease of the core–core association between the HBFPs would be observed, resulting in MCMs of small sizes. In this study, we designed and synthesized a series of hyperbranched polymers having the same hydrophobic HBFP core and different lengths and numbers of PEO arms. The self-assembly and formation of MCMs from these PEO-functionalized HBFPs were then investigated.

EXPERIMENTAL

Materials

All chemicals were purchased from Sigma-Aldrich, unless otherwise noted. Poly(ethylene oxide) amine (PEO_x-NH_2, x = 15, 44, and 112 for M_n = 750, 2000, and 5000 Da) was purchased from Interzyne (Tampa, FL) and used without further purification.

Characterization Methods

IR spectra were obtained on a Perkin-Elmer Spectrum BX Fourier-transform infrared (FTIR) spectrometer using NaCl plates, with the sample being deposited from CH_2Cl_2 and allowing for evaporation of the solvent.

^{1}H NMR spectra were recorded at 300 or 500 MHz on a Varian Unity-plus 300 or Varian Inova 500 spectrometer, respectively, with the solvent proton signal as standard. ^{13}C NMR spectra were recorded at 125 MHz on a Varian Inova 500 spectrometer, with the solvent carbon signal as standard. ^{19}F NMR spectra were recorded at 470 MHz on a Varian Inova 500 spectrometer with CF_3COOH as an external standard.

Gel permeation chromatography (GPC) was conducted on a Waters 1515 HPLC (Waters Chromatography) equipped with a Waters 2414 differential refractometer and a three-column series PL gel 5 μm Mixed C, 500 Å, and 10^4 Å, 300 mm × 7.5 mm columns (Polymer Laboratories). The system was equilibrated at 35 °C in stabilized THF, which served as the polymer solvent and eluent with a flow rate of 1.0 mL min^{-1}. Polymer solutions were prepared at a known concentration (ca. 3 mg mL^{-1}), and an injection volume of 200 μL was used. Data collection and analyses were performed with Precision Acquire software and Discovery 32 software, respectively (Precision Detectors).

Thermogravimetric analysis (TGA) was performed on a TGA/SDTA851 instrument (Mettler-Toledo) measuring the total mass loss on about 5 mg samples from 25 to 550 °C at a heating rate of 10 °C min^{-1} in a nitrogen flow of 50 mL min^{-1}. Glass transition temperature (T_g) determinations were measured by differential scanning calorimetry (DSC) on a DSC822 instrument (Mettler-Toledo) in a temperature range of −75 to 150 °C with a heating rate of 10 °C min^{-1} under nitrogen. For both TGA and DSC, data were acquired and analyzed with STAR^e software (Mettler-Toledo). The T_g values were taken at the midpoint of the inflection tangent, and T_m values were taken as the onset, upon the third heating scans.

Dynamic light scattering (DLS) measurements were acquired using a Brookhaven Instruments (Worcestershire, UK) system, including a model BI-200SM goniometer, a model BI-9000AT digital correlator, a model EMI-9865 photomultiplier, and a model 95-2 Ar ion laser (Lexel Corp., Farmindale, NY) operated at 514.5 nm. Measurements were made at 25 ± 1 °C. Before analysis, solutions were filtered through a 0.45-μm Gelman Nylon Acrodisc® 13 membrane filter to remove dust particles. Scattered light was collected at a fixed angle of 90°. The digital correlator was operated with 522 ratio spaced channels, and initial delay of 5 μs, a final delay of 100 ms, and a duration of 10 min. A photomultiplier aperture of 400 μm was used, and the incident laser intensity was adjusted to obtain a photon counting of between 200 and 300 kcps. The calculations of the particle size distributions and distribution averages were performed with the

ISDA software package (Brookhaven Instruments), which used CONTIN particle size distribution analysis. The data are presented as the average values from four measurements.

Transmission electron microscopy (TEM) measurements were conducted on a Hitachi H600 microscope. Micrographs were collected at 100,000× magnification and calibrated using a 41-nm polyacrylamide bead from NIST. Carbon-coated copper grids were treated with oxygen plasma before deposition of the micellar samples. The samples were deposited on the carbon grids for 1 min, and excess samples were wicked away. The samples were stained with 1% phosphotungstic acid for 1 min; excess stain solution was wicked away, and the samples were allowed to dry under ambient conditions. The number-average particle diameters (D_{av}) and standard deviations were generated from the analysis of a minimum of 100 particles from at least three different micrographs.

Elemental analyses were conducted by Galbraith Laboratories (Knoxville, TN).

Synthesis of 1-(4′-(Hydroxymethyl)benzyloxy)-2,3,5,6-tetrafluoro-4-vinylbenzene (2)

To a solution of 1,4-benzenedimethanol (**1**, 9.4 g, 68 mmol) in THF (200 mL) was added NaH (1.6 g, 68 mmol) at 0 °C. 2,3,4,5,6-Pentafluorostyrene (PFS, 12 g, 62 mmol, in 100 mL THF) was added dropwise through an addition funnel over a period of 12 h. The reaction was stirred under argon at room temperature overnight. H_2O (100 mL) and EtOAc (100 mL) were added, and the aqueous solution was extracted with EtOAc (3 × 100 mL). The organic solutions were combined and dried over anhydrous sodium sulfate. The solvent was removed under reduced pressure, and the residues were purified by silica gel column chromatography (hexanes/EtOAc = 7/3 v/v) to give **2** as a white powder (12.6 g, 65%).

FTIR (NaCl): 3246, 2918, 1647, 1489, 1382, 1149, 964 cm^{-1}. ^1H NMR (500 MHz, $CDCl_3$) δ: 4.58 (s, 2H, Ar***CH₂***OH,), 5.23 (s, 2H, $ArCH_2O$-ArF_4), 5.61 (d, J = 12.0 Hz, 1H, *cis* CH=C***H₂***), 6.00 (d, J = 18.0 Hz, 1H, *trans* CH=C***H₂***), 6.59 (dd, J = 18.0, 12.0 Hz, 1H, C***H***=CH_2), 7.30 (1/2 AB_q, J = 8.0 Hz, 2H, Ar***H***), 7.40 (1/2 AB_q, J = 8.0 Hz, 2H Ar***H***) ppm. ^{13}C NMR (125.7 MHz, $CDCl_3$) δ: 64.7, 76.2, 111.1, 121.9, 122.3, 122.4, 127.0, 128.6, 134.9, 141.4 (d, J = 250 Hz), 145.1 (d, J = 250 Hz) ppm. ^{19}F NMR (282 MHz, $CDCl_3$ with CF_3COOH as an external reference) δ: 46.48 (s, 2F), 57.10 (s, 2F) ppm. Elem. Anal. Calcd. for $C_{16}H_{12}F_4O_2$: C, 61.54%; H, 3.87%; F, 24.34%; found: C, 61.41%; H, 3.82%; F, 24.90%.

Synthesis of 1-(4′-(Bromomethyl)benzyloxy)-2,3,5,6-tetrafluoro-4-vinylbenzene (3)

To a solution of **2** (6.6 g, 21 mmol) in CH_2Cl_2 (100 mL) was added Ph_3P (11.0 g, 42 mmol) and CBr_4 (20.8 g, 63 mmol). The reaction was allowed to stir at room temperature for 4 h. The solvent was removed under reduced pressure, and the residue was purified by silica gel column chromatography (hexanes/EtOAc = 8/2, v/v) to give **3** as a white powder (5.5 g, 70%).

FTIR (NaCl): 2916, 1629, 1486, 1438, 1404, 974, 958 cm^{-1}. ^1H NMR (300 MHz, $CDCl_3$) δ: 4.51 (s, 2H, Ar***CH₂***Br), 5.26 (s, 2H, Ar***CH₂***O-ArF_4), 5.65 (d, J = 12.0 Hz, 1H, *cis* CH=C***H₂***), 6.05 (d, J = 18.0 Hz, 1H, *trans* CH=C***H₂***), 6.59 (dd, J = 18.0, 12.0 Hz, 1H, C***H***=CH_2), 7.44 (m, 4H, Ar***H***) ppm. ^{13}C NMR (75 MHz, $CDCl_3$) δ 32.81, 75.8, 111.1, 122.0, 122.3, 122.4, 128.5, 128.8, 128.9, 135.9, 138.4, 141.2 (d, J = 250 Hz), 145.0 (d, J = 250 Hz) ppm. ^{19}F NMR (282 MHz, $CDCl_3$): δ 46.55 (s, 2F), 57.21 (s, 2F) ppm. Elem. Anal. Calcd. for $C_{16}H_{11}BrF_4O$: C, 51.22%; H, 2.96%; Br, 21.30%; F, 20.26%; found: C, 51.46%; H, 2.93%; Br, 20.97%; F, 21.04%.

Synthesis of HBFP (4)

To a solution of **3** (3.0 g, 8 mmol) in PhF (15 mL) in a Schlenk flask was added bipyridine (1.8 g, 0.22 mmol). After one cycle of freeze-pump-thaw, CuCl (79 mg, 0.80 mmol) and $CuCl_2$ (11 mg, 0.08 mmol) were added. The reaction mixture was subjected to three additional freeze-pump-thaw cycles and placed in an oil bath set at 65 °C. After 8 h, the reaction was quenched by immersion of the reaction flask into a liquid N_2 bath. The copper catalysts were removed by filtration of the reaction mixture through a short plug of basic alumina. The solvent was removed under reduced pressure, and the polymer was purified by precipitation into hexanes (3 × 1000 mL). The polymer was collected by centrifugation (3000 rpm × 5 min) to give HBFP **4** as an off-white powder (1.6 g, 53% based on mass). M_n^{GPC} = 28 kDa, M_w/M_n^{GPC} = 2.1.

FTIR (NaCl): 2945, 1648, 1458, 1420, 1376, 1225, 1140, 1086, 960 cm^{-1}. ^1H NMR (500 MHz, $CDCl_3$) δ: 0.8–3.1 (br, m, ***CH₂*** and ***CH*** of backbone), 4.4–4.6 (m, Ar***CH₂***Br), 4.9–5.4 (m, br, Ar***CH₂***O-ArF_4), 6.9–7.4 (m, br, Ar***H***) ppm. ^{13}C NMR (125.7 MHz, $CDCl_3$) δ: 31.5–40.5, 75.9, 116.4–118.6, 128.4–129.3, 135.7–146.3 ppm. ^{19}F NMR (282 Hz, $CDCl_3$) δ: 46.8 (m, br), 57.3 (m, br) ppm. Elem. Anal. Calcd. for $(C_{16}H_{11}BrF_4O)_{75}$: C, 51.22%; H, 2.96%; Br, 21.30%; F, 20.26%; found: C, 51.07%; H, 2.89%; Br, 17.01%; Cl, 1.29%; F, 20.24%. DSC: T_g = 56 °C; TGA: 25–220 °C, ∼0% mass loss; 220–280 °C, 22% mass loss; and 280–450 °C, 47% mass loss.

Synthesis of $(PEO_x)_y$-HBFPs (5a–5e)

To five separate solutions of **4** (100 mg, 0.26 mmol Br) in CH_2Cl_2 (30 mL) was added PEO_{15}-NH_2 (0.10, 0.08, and 0.06 mmol, 75, 60, and 45 mg each for **5a**, **5b**, and **5c**, respectively), PEO_{43}-NH_2 (0.06 mmol, 120 mg for **5d**), and PEO_{112}-NH_2 (0.06 mmol, 300 mg for **5e**). Diisopropylethyl amine (DIPEA, 100 mg, 0.78 mmol) was added to each reaction, and the reaction mixtures were allowed to stir under argon at room temperature for 72 h. The solvent was removed under reduced pressure, and the residues were precipitated into hexanes/ethyl acetate (8/2, v/v) to give **5a–5e** as off-white powders.

5a: 99 mg (56%). M_n^{NMR} = 48 kDa. FTIR (NaCl): 2918, 2849, 2362, 1647, 1492, 1459, 1348, 1259, 1100 cm^{-1}. ^1H NMR (500 MHz, $CDCl_3$) δ: 0.8–3.1 (br, m, ***CH₂*** and ***CH*** of backbone), 3.2–3.3 (s, br, PEO-O***CH₃***), 3.5–3.8 (m, br, PEO-***H***), 4.5–4.6 (s, br, Ar***CH₂***Br), 4.9–5.4 (m, Ar***CH₂***O-ArF_4), 6.9–8.1 (m,

br, Ar***H***) ppm. ^{19}F NMR (282 Hz, $CDCl_3$) δ: 46.9 (m, br), 57.5 (m, br) ppm. ELEM. ANAL. Calcd. for $C_{2157}H_{2797}Br_{46}F_{300}N_{29}O_{539}$ (47 kDa): C, 55.78%; H, 6.01%; F, 12.21%; found: C, 55.95%; H, 6.04%; F, 12.09%. DSC: T_m = 50 °C; TGA: 25–230 °C, ~0% mass loss; 230–380 °C, 22% mass loss; and 380–460 °C, 62% mass loss.

5b: 106 mg (66%). M_n^{NMR} = 44 kDa. FTIR (NaCl): 2917, 2849, 1648, 1492, 1459, 1348, 1260, 1101 cm^{-1}. ^{1}H NMR (500 MHz, $CDCl_3$) δ: 0.9–3.1 (br, m, ***CH$_2$*** and ***CH*** of backbone), 3.2–3.3 (s, br, PEO-O***CH$_3$***), 3.5–3.9 (m, br, PEO-***H***), 4.4–4.7 (s, br, Ar***CH$_2$***Br), 4.9–5.4 (m, Ar***CH$_2$***O-ArF_4), 6.9–8.0 (m, br, Ar***H***) ppm. ^{19}F NMR (282 Hz, $CDCl_3$) δ: 46.8 (m, br), 57.4 (m, br) ppm. ELEM. ANAL. Calcd. for $C_{1926}H_{2321}Br_{53}F_{300}N_{22}O_{427}$ (43 kDa): C, 54.37%; H, 5.50%; F, 13.40%; found: C, 54.84%; H, 5.70%; F, 12.56%. DSC: T_m = 45 °C; TGA: 25–230 °C, ~0% mass loss; 230–330 °C, 10% mass loss; and 330–420 °C, 68% mass loss.

5c: 101 mg (69%). M_n^{NMR} = 40 kDa. FTIR (NaCl): 2920, 2940, 1649, 1492, 1458, 1348, 1259, 1100, 1060 cm^{-1}. ^{1}H NMR (500 MHz, $CDCl_3$) δ: 0.8–3.1 (br, m, ***CH$_2$*** and ***CH*** of backbone), 3.2–3.4 (s, br, PEO-O***CH$_3$***), 3.5–3.8 (m, br, PEO-***H***), 4.4–4.6 (s, br, Ar***CH$_2$***Br), 4.9–5.4 (m, Ar***CH$_2$***OArF), 6.9–8.0 (m, br, Ar***H***) ppm. ^{19}F NMR (282 Hz, $CDCl_3$) δ: 46.8 (m, br), 57.5 (m, br) ppm. ELEM. ANAL. Calcd. for $C_{1728}H_{1913}Br_{59}F_{300}N_{16}O_{331}$ (39 kDa): C, 53.75%; H, 4.99%; F, 14.76%; found: C, 54.04%; H, 5.20%; F, 13.96%. DSC: T_m = 39 °C; TGA: 25–110 °C, ~0% mass loss; 110–240 °C, 17% mass loss; 240–380 °C, 26% mass loss; and 380–420 °C, 65% mass loss.

5d: 116 mg (53%). M_n^{NMR} = 59 kDa. FTIR (NaCl): 3503, 2917, 2849, 1648, 1492, 1459, 1348, 1260, 1101 cm^{-1}. ^{1}H NMR (500 MHz, $CDCl_3$) δ: 0.9–3.1 (br, m, ***CH$_2$*** and ***CH*** of backbone), 3.2–3.3 (s, br, PEO-O***CH$_3$***), 3.5–3.9 (m, br, PEO-***H***), 4.4–4.7 (s, br, Ar***CH$_2$***Br), 4.9–5.4 (m, Ar***CH$_2$***O-ArF_4), 6.9–8.1 (m, br, Ar***H***) ppm. ^{19}F NMR (282 Hz, $CDCl_3$) δ: 46.7 (m, br), 57.3 (m, br) ppm. ELEM. ANAL. Calcd. for $C_{2656}H_{3769}Br_{59}F_{300}N_{16}O_{795}$ (59 kDa): C, 54.02%; H, 6.43%; F, 9.65%; found: C, 54.88%; H, 6.61%; F, 9.07%; DSC: T_m = 52 °C; TGA: 25–230 °C, ~0% mass loss; 230–330 °C, 10% mass loss; and 330–420 °C, 68% mass loss.

5e: 148 mg (37%). M_n^{NMR} = 108 kDa. FTIR (NaCl): 2920, 2940, 1649, 1492, 1458, 1348, 1259, 1100, 1060 cm^{-1}. ^{1}H NMR (500 MHz, $CDCl_3$) δ: 0.8–3.1 (br, m, ***CH$_2$*** and ***CH*** of backbone), 3.2–3.4 (s, br, PEO-O***CH$_3$***), 3.5–3.9 (m, br, PEO-***H***), 4.4–4.6 (s, br, Ar***CH$_2$***Br), 4.9–5.4 (m, Ar***CH$_2$***OArF), 6.9–8.1 (m, br, Ar***H***) ppm. ^{19}F NMR (282 Hz, $CDCl_3$) δ: 46.8 (m, br), 57.5 (m, br) ppm. ELEM. ANAL. Calcd. for $C_{4832}H_{8121}Br_{59}F_{300}N_{16}O_{1883}$ (103 kDa): C, 54.25%; H, 7.65%; F, 5.33%; found: C, 54.84%; H, 7.70%; F, 4.66%; DSC: T_m = 56 °C; TGA: 25–110 °C, ~0% mass loss; 110–240 °C, 17% mass loss; 240–380 °C, 26% mass loss; and 380–420 °C, 65% mass loss.

Formation of Micelles of 5a–5e

$(PEO_x)_y$-HBFPs (**5a–5e**, 25 mg each) were dissolved in *N,N*-dimethyl formamide (DMF, 25 mL) to make solutions with concentration of 1 mg mL^{-1}. The solutions were stirred at room temperature for 2 h. Nanopure water (25 mL) was added dropwise to each solution over a period of 3 h. The solutions were stirred for another 4 h and then dialyzed against nanopure water for 72 h to afford the micelle solutions.

5a micelles: 0.30 mg mL^{-1}. TEM: D_{av}: 13 ± 4 nm, DLS: $D_{h(n)}$: 20 ± 5 nm; $D_{h(v)}$: 29 ± 4 nm; $D_{h(i)}$: 150 ± 30 nm.

5b micelles: 0.32 mg mL^{-1}. TEM: D_{av}: 19 ± 6 nm; DLS: $D_{h(n)}$: 22 ± 5 nm, $D_{h(v)}$: 29 ± 5 nm, and $D_{h(i)}$: 230 ± 40 nm.

5c micelles: 0.30 mg mL^{-1}. TEM: D_{av}: 28 ± 5 nm; DLS: $D_{h(n)}$: 32 ± 5 nm, $D_{h(v)}$: 35 ± 6 nm, and $D_{h(i)}$: 350 ± 60 nm.

5d micelles: 0.31 mg mL^{-1}. TEM: D_{av}: 16 ± 3 nm; DLS: $D_{h(n)}$: 24 ± 3 nm, $D_{h(v)}$: 28 ± 3 nm, and $D_{h(i)}$: 210 ± 30 nm.

5e micelles: 0.29 mg mL^{-1}. TEM: D_{av}: 12 ± 2 nm; DLS: $D_{h(n)}$: 19 ± 5 nm, $D_{h(v)}$: 27 ± 5 nm, and $D_{h(i)}$: 150 ± 40 nm.

RESULTS AND DISCUSSION

The synthetic strategy for the preparation of amphiphilic $(PEO_x)_y$-HBFPs involved the construction of HBFP as a core unit by ATR-SCVP, followed by covalent attachment of PEO chains via nucleophilic substitution of benzylic halide functionalities on HBFP with amine-functionalized PEO. The aggregation behaviors of the resulting $(PEO_x)_y$-HBFPs upon transitioning from organic solvent to water were then investigated as a function of chain length and grafting number of the PEO arms.

Synthesis of HBFP 4

The synthesis of HBFP involved the preparation and polymerization of inimer **3** (Scheme 1). Nucleophilic substitution of PFS with an excess of 1,4-benzenedimethanol (**1**) was conducted in the presence of NaH in THF to give mono-substituted **2** as the major product. The hydroxyl group present in **2** was subsequently converted to a bromide functionality using Ph_3P/CBr_4 to afford **3** in 70% yield. ATR-SCVP of inimer **3** was performed according to the protocol reported previously.[57] The polymerization was monitored by GPC and ^{1}H NMR analysis. As expected, the GPC traces (Fig. 1) illustrated an increase in molecular weight along the reaction time. The kinetic data showed a steady increase of molecular weight upon reaction time (Fig. 2), with a parallel increase in the PDI values of the resulting polymers. As a typical behavior for ATR-SCVP, along with the increase of inimer conversion, the average molecular weight increases sharply because of the combined addition- and step-growth polymerization processes, which in turn implies the formation of a hyperbranched structure.[58]

Syntheses of $(PEO_x)_y$-HBFPs (5a–5e)

PEO chains in different lengths and numbers were conjugated onto **4** by taking advantage of the large number of benzylic halide groups (ca. 75 Br/Cl readily available on each HBFP, based on ^{1}H NMR spectroscopy and elemental analysis). The alkylation reactions were first conducted using equal molar equivalents of the benzyl halide moiety and PEO_x-NH_2 in the presence of DIPEA in CH_2Cl_2 to test the

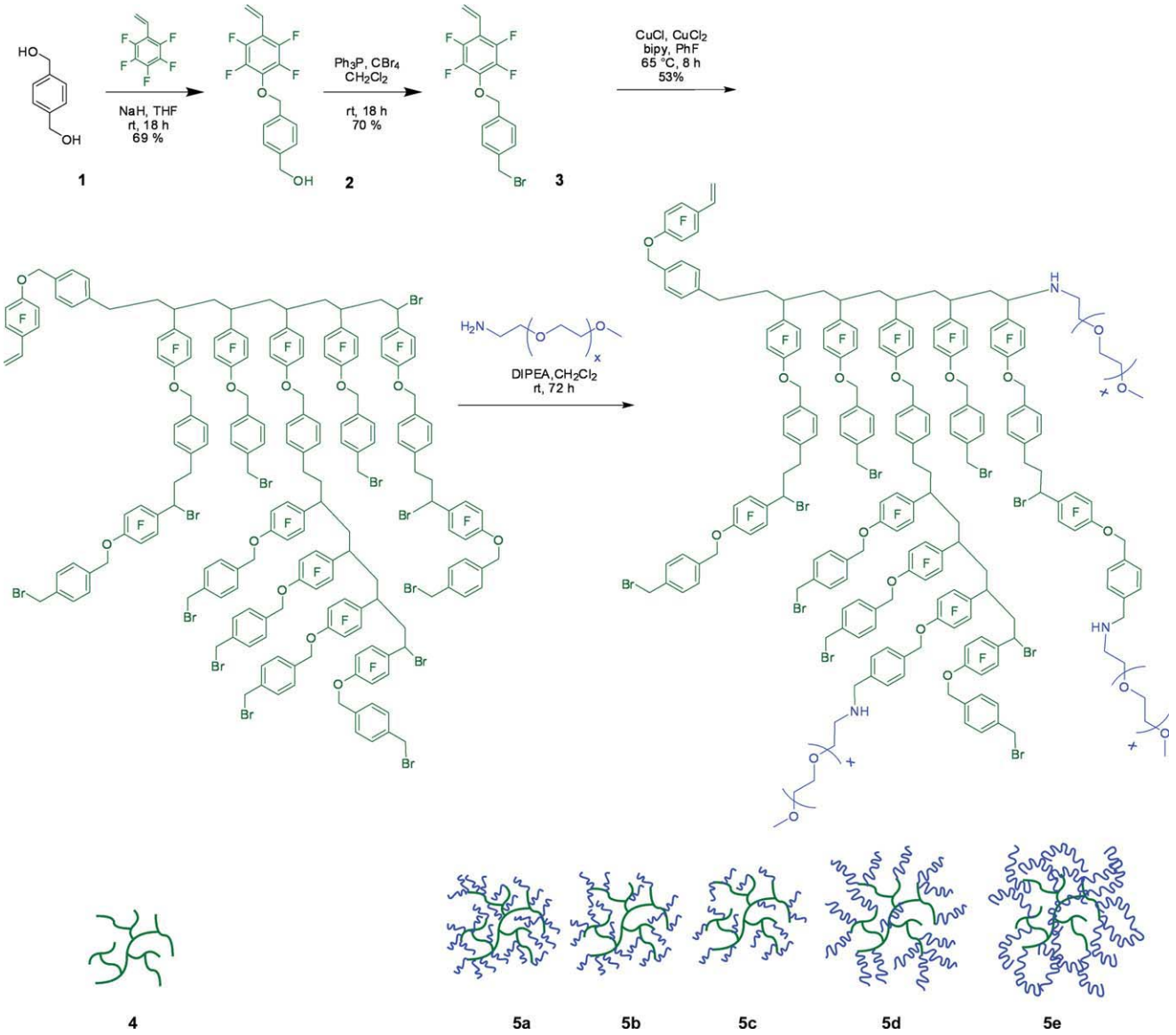

SCHEME 1 Synthetic route for the preparation of $(PEO_x)_y$-HBFPs **5a–5e** with illustrations that show the pictorial representation of HBFP **4**, and the $(PEO_x)_y$-grafted polymers **5a–5e**. The green, branched structure depicts a single molecule of the HBFP precursor **4**, whereas the blue, wavy lines illustrate the functionalization of **4** with various lengths and amounts of PEO to produce **5a–5e**.

reaction efficiency. Only a portion of PEO_x-NH_2 was able to attach to the HBFP core, and the reaction efficiency decreased as the length of the PEO_x-NH_2 increased (39, 29, and 22% for PEO_{15}-NH_2, PEO_{44}-NH_2, and PEO_{112}-NH_2, respectively), presumably because of steric hindrance. Efforts to increase the extent of alkylation, by either an increase in PEO_x-NH_2 feed or an increase in reaction time, did not significantly improve the degree of substitution, suggesting that the reaction may be limited to only the surface available alkyl halides. It was found that an average of 29 short PEO_{15} could be coupled onto **4**, whereas only about 16 PEO_{112} chains could be grafted onto **4**. Therefore, the breadth in the chain numbers and chain lengths provided for a systematic investigation of the effects of each of the supramolecular assembly of these amphiphilic hybrid branched-star polymers in water. Comparisons were made between **5a**, **5b**, and **5c**, having 29, 22, and 16 PEO arms, respectively, to determine the effects of the PEO grafting density, and between **5c**, **5d**, and **5e**, having 16 arms of PEO_{15}, PEO_{44}, and PEO_{112}, respectively, to evaluate the effects of the PEO length (Scheme 1).

The synthesized $(PEO_x)_y$-HBFPs (**5a–5e**) were characterized by ^1H NMR and ^{19}F NMR spectroscopy, IR, elemental analysis, and GPC analysis. Attempts to characterize the synthesized $(PEO_x)_y$-HBFPs by GPC were not successful, except for the polymer having the lowest grafting density of the shortest PEO chains, **5c**, because of the low solubility of $(PEO_x)_y$-HBFPs in THF (less than 1 mg mL^{-1}). Even in other organic solvents (such as CH_2Cl_2), these $(PEO_x)_y$-HBFPs self-assembled to form gel-like materials, as also observed by

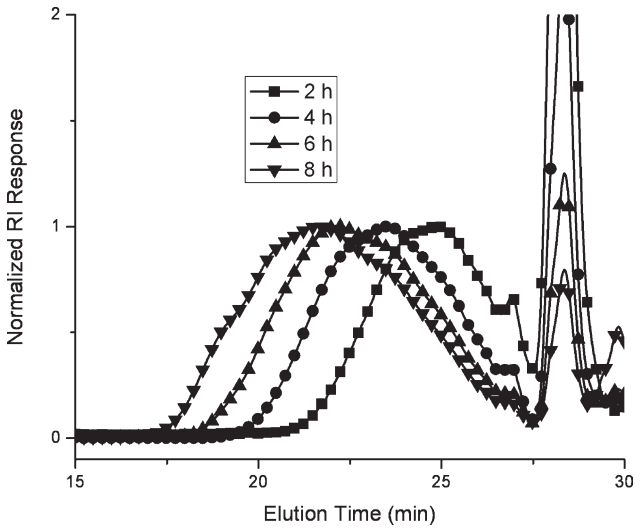

FIGURE 1 GPC traces of ATR-SCVP of monomer **3** to yield HBFP **4**, ($[\mathbf{3}]_0/[CuCl]_0/[CuCl_2]_0/[bipy]_0$ = 1.0/0.1/0.01/0.22, PhF, 65 °C).

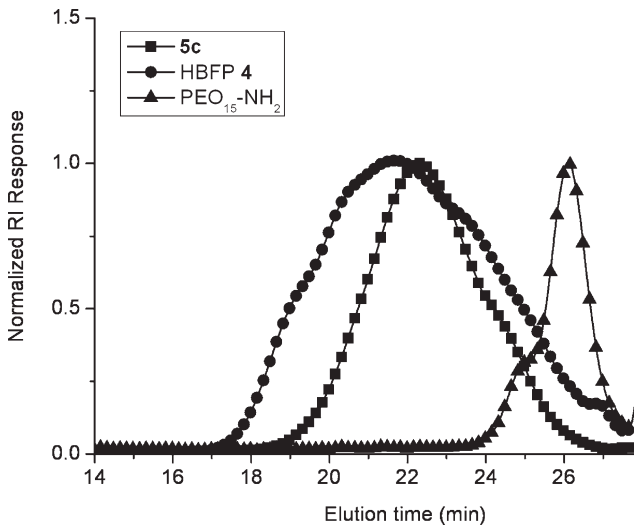

FIGURE 3 GPC traces (THF, 1.0 mL min^{-1}) for PEO_{15}-NH_2 (M_n = 750 Da), HBFP **4**, and $(PEO_{15})_{16}$-HBFP **5c**.

other groups.[59] Even for **5c**, the molecular weight when determined by GPC was found to be lower than the data obtained by ^{1}H NMR spectroscopy, because of the poor solubility in THF, resulting in a collapse of the polymers and smaller apparent molecular weights than expected. In fact, the retention time for $(PEO_{15})_{16}$-HBFP (**5c**) was longer than that of the starting core material **4** (Fig. 3). No free PEO chains were observed for GPC curve of **5c**, indicating that the purification by precipitation into hexanes/ethyl acetate removed nonconjugated PEO chains. Therefore, ^{1}H NMR, ^{19}F NMR, and elemental analysis could be used to determine the average numbers of PEO arms grafted onto each HBFP core, relying on the GPC-derived molecular weight of **4**.

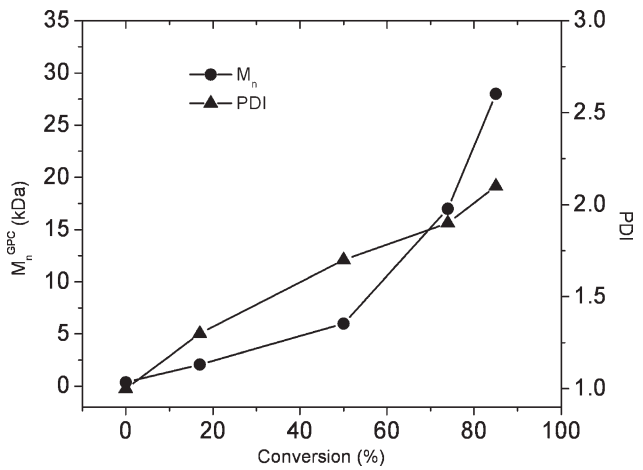

FIGURE 2 Plots of molecular weight versus conversion (●) and PDI versus conversion (▲), indicating the sharp increase of M_n after about 50% conversion, and progressively increasing PDI values.

A representative ^{1}H NMR spectrum of **5c** is shown in Figure 4. The appearance of a resonance at 3.2–3.8 ppm and the reduction in the benzylic halide protons of the grafted amphiphilic structures, in comparison to those of 4, indicated the conjugation of PEO units to the HBFP **4**. Based on the $(PEO_x)_y$-HBFP structures analyzed by ^{1}H NMR spectroscopy, it was calculated that the M_n values were 48, 44, 40, 60, and 108 kDa for polymers **5a**–**5e**, respectively, starting from a M_n value of 29 kDa for HBFP **4**. The experimental elemental analysis data were in good agreement with the calculated values for these structures.

The ^{19}F NMR spectra of **3**, **4**, and representative **5c** are shown in Figure 5. There were two broad peaks observed at 46 and 57 ppm, representing the *meta*-(F^a) and *ortho*-(F^b) fluorine atoms, respectively. PEO attachment, as expected, did not have any impact in the chemical shifts of the fluorine nuclei. The integration values for these two peaks were maintained at a ratio of 1:1. Both NMR and elemental analysis suggest that there was no fluorine loss in the PEGylation reaction. The peak widths were about 800 Hz, significantly narrower than that of TEG-functionalized HBFPs previously reported (ca. 2000 Hz).[43] The narrow ^{19}F resonance may allow these $(PEO_x)_y$-HBFPs to serve as ^{19}F imaging agents.

Micelle Formation

The amphiphilic $(PEO_x)_y$-functionalized HBFPs, containing a hydrophobic core and a hydrophilic PEO shell, were found to readily form micelles in water. The resulting micelles were characterized by TEM and DLS. The uniform, circular two-dimensional objects having average diameters of 13 ± 4, 19 ± 6, 28 ± 6, 16 ± 3, and 12 ± 2 nm for micelles derived from **5a**–**5e**, respectively, observed by TEM (Fig. 6) suggest that the micelles were uniform, globular assemblies. The number-averaged hydrodynamic diameter values ($(D_h)_n$), 20 ± 5, 22 ± 5, 32 ± 5, 24 ± 3, and 19 ± 5 nm for micelles

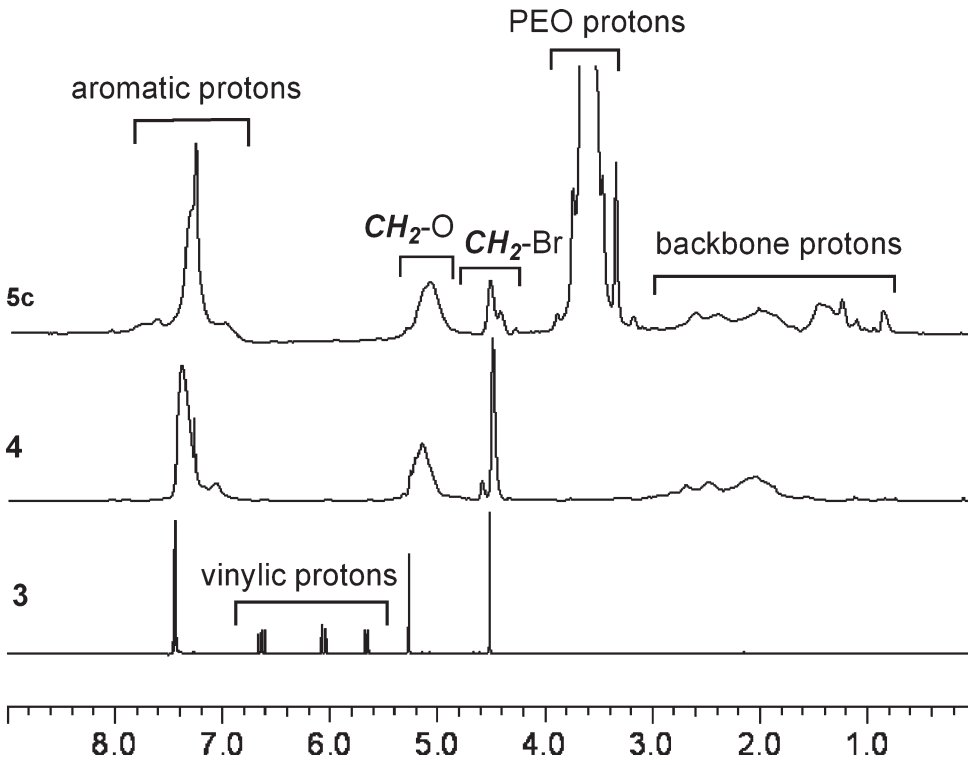

FIGURE 4 ^{1}H NMR (300 MHz, $CDCl_3$) spectra of inimer **3**, HBFP **4**, and $(PEO_{15})_{16}$-HBFP **5c**.

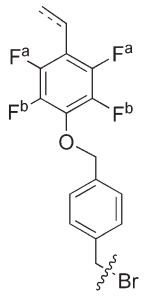

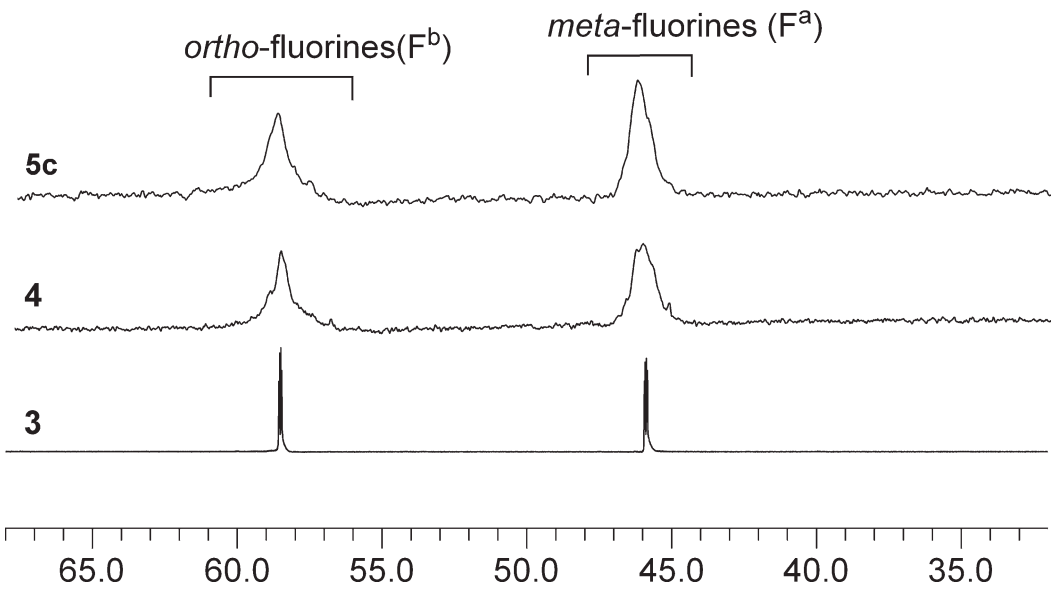

FIGURE 5 ^{19}F NMR spectra of **3**, **4**, and **5c** (282 MHz, $CDCl_3$ with CF_3COOH as an external reference).

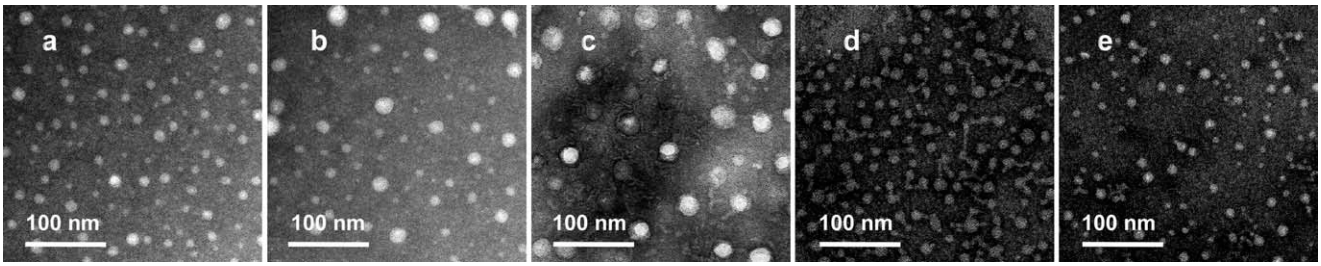

FIGURE 6 TEM images of micelles **5a–5e** (1% phosphotungstic acid negative stain).

derived from **5a–5e**, respectively, measured by DLS (Fig. 7), were in good agreement with the dry-state TEM diameters, taking into consideration swelling by water. However, the intensity-averaged hydrodynamic diameter values ($(D_h)_i$), 150 ± 30, 230 ± 40, 350 ± 60, 210 ± 30, and 150 ± 40 nm for micelles derived from **5a–5e**, respectively, were unexpectedly large, suggesting there were large micelles formed. Because ($(D_h)_i$) values are very sensitive to large-size particles, a small amount of large particles can lead to a large increase in ($(D_h)_i$) values. Although we did not observe large micelles in the TEM studies, DLS data indicated that they did exist, possibly because of multiple micelle–micelle aggregation, as observed by Mao et al.[44]

The micellar assemblies were believed to be the result of multimolecular aggregation of $(PEO_x)_y$-HBFPs. The aggregation numbers (Table 1) can be calculated to be 16, 54, 190, 24, and 6 for **5a–5e**, respectively, according to the published method.[60] Because of the strong hydrophobic interactions between the fluoropolymer components, high aggregation numbers were obtained when the numbers of PEO units were low, as illustrated by the trend in size observed from **5a–5c**, whereby each polymer has the same PEO chain length but decreasing grafted PEO densities. Similarly, increased PEO chain lengths led to decreased aggregation numbers and smaller supramolecular assemblies, **5c** versus **5d** versus **5e**.

Supramolecular attractions of the HBFP cores, based upon hydrophobic effects and π–π stacking interactions, are expected to be the dominant factor to drive the aggregation of $(PEO_x)_y$-HBFPs. However, as these results suggested, the surface PEO units can serve as a shielding layer to diminish the HBFP core–core attractions. In our initial investigation of preparation and micelle formation, amphiphilic HBFPs were synthesized via ATR-SCVP of a PEO-functionalized inimer with an integrated tri(ethylene oxide) unit. The micelles derived from such HBFPs gave $(D_h)_n$ of 170–190 nm.[43] Even though the PEO wt % was 32%, comparable to that of **5b** (wt % = 33%, Table 1), the size of the micelles in the parent study was significantly larger than that derived from **5b** ($(D_h)_n$ = 22 nm, Table 1), indicating that the PEO shielding effect is more pronounced when the PEOs are attached as mono-attached grafts onto the HBFP framework, to give a star-like structure, rather than incorporated as many short units within the HBFP matrix.

CONCLUSIONS

In summary, a series of $(PEO_x)_y$-HBFPs, which share the same HBFP core but differ in the grafting numbers and chain lengths of PEO arms, have been designed and synthesized. These amphiphilic macromolecules were found to readily form micelles upon transitioning from organic solvent to water. The particle sizes, determined by TEM and DLS, decreased as the grafting numbers or the chain lengths of PEO_x increased, suggesting an increase in the PEO shielding effect and a reduction in the HBFP core–core interactions. Based upon comparisons to seminal studies from which this work is derived, the effect of PEO shielding is greater when the PEO arms are grafted onto the HBFP core through attachment of one PEO end, rather than being integrated as short segments locked within the HBFP matrix by coupling of both ends of short oligomers. These $(PEO_x)_y$-HBFPs could be potentially useful in biomedical applications as ^{19}F magnetic resonance imaging agents and therapeutic delivery vehicles. The high grafting densities of PEO chains may allow the application of these nanostructures in biomedical research to resist nonspecific protein adsorption and to limit opsonization and clearance by the mononuclear phagocytic system.[61] Such studies and potential applications are currently being explored.

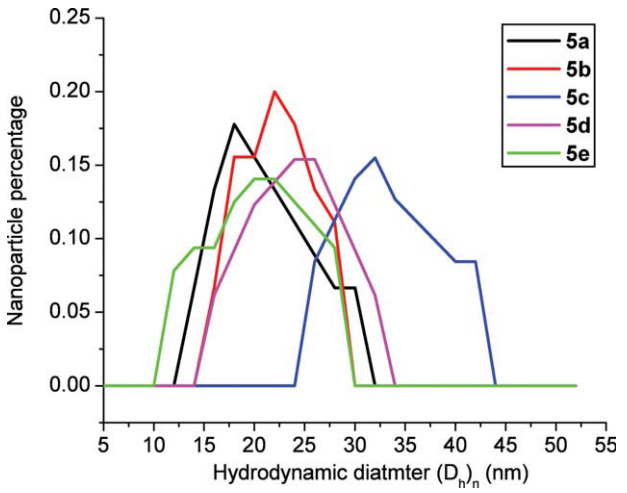

FIGURE 7 Number-averaged hydrodynamic diameter $(D_h)_n$ size distributions of the micelles as determined by DLS.

TABLE 1 $(PEO_x)_y$-HBFPs **5a–5e** and Their Characterization Data

	5a	5b	5c	5d	5e
M_n of HBFP core (kDa)[a]	29	29	29	29	29
x value	15	15	15	44	112
y value	29	22	16	16	16
PEO units/HBFP[b]	435	330	240	704	1792
M_n of total PEO units (kDa)[a]	19	15	11	31	79
M_n of $(PEO_x)_y$-HBFP (kDa)	48	44	40	60	108
Wt % of PEO	40%	33%	27%	52%	73%
D_{av} (TEM, nm)	13 ± 4	19 ± 6	28 ± 5	16 ± 3	12 ± 2
$(D_h)_n$ (DLS, nm)	20 ± 5	22 ± 5	32 ± 5	24 ± 3	19 ± 5
$(D_h)_v$ (DLS, nm)	29 ± 4	29 ± 5	35 ± 6	28 ± 3	27 ± 5
$(D_h)_i$ (DLS, nm)	150 ± 30	230 ± 40	350 ± 60	210 ± 30	150 ± 40
Volume per aggregate (nm^3)[c]	1150	3589	11,488	2143	904
Volume per $(PEO_x)_y$-HBFP (nm^3)[d]	80	72	66	100	179
Aggregation number[e]	16	54	190	24	6

[a] Based on ^{1}H NMR data.
[b] PEO units/HBFP = $x \times y$.
[c] Based on TEM diameters and $V = 4/3(\pi r^3)$.
[d] Volume per $(PEO_x)_y$-HBFP = (M_n/Avogadro's number)/density of PEO (1.1 g mL^{-1}).
[e] Aggregation number = (volume per aggregate)/(volume per PEO_x-HBFP).

The authors thank G. Michael Veith (Washington University Electron Microscopy Laboratory) for assistance with TEM. Postdoctoral and assistant professor fellowships provided by the Knut and Alice Wallenberg Foundation (A. M. Nyström) and Niko Foundation (W. Du) are gratefully acknowledged. This material is based upon work supported by the National Heart Lung and Blood Institute of the National Institutes of Health as a Program of Excellence in Nanotechnology (HL080729), the Children's Discovery Institute of Washington University in Saint Louis, and the Office of Naval Research (N00014-08-1-0398).

REFERENCES AND NOTES

1 Husemann, M.; Mecerreyes, D.; Hawker, C. J.; Hedrick, J. L.; Shah, R.; Abbott, N. L. Angew Chem Int Ed 1999, 38, 647–649.

2 Thurn-Albrecht, T.; Steiner, R.; DeRouchey, J.; Stafford, C. M.; Huang, E.; Bal, M.; Tuominen, M.; Hawker, C. J.; Russell, T. P. Adv Mater 2000, 12, 787–791.

3 Black, C. T. ACS Nano 2007, 1, 147–150.

4 Cheng, J. Y.; Ross, C. A.; Smith, H. I.; Thomas, E. L. Adv Mater 2006, 18, 2505–2521.

5 Hawker, C. J.; Russell, T. P. MRS Bull 2005, 30, 952–966.

6 Li, M.; Ober, C. K. Mater Today 2006, 9, 30–39.

7 Stoykovich, M. P.; Kang, H.; Daoulas, K. C.; Liu, G.; Liu, C.-C.; de Pablo, J. J.; Müller, M.; Nealy, P. F. ACS Nano 2007, 1, 168–175.

8 Torchilin, V. P. Cell Mol Life Sci 2004, 56, 2549–2559.

9 Ahmed, F.; Pakunlu, R. I.; Srinivas, G.; Brannan, A.; Bates, F.; Klein, M. L.; Minko, T.; Discher, D. E. Mol Pharm 2006, 3, 340–350.

10 Torchilin, V. P. Pharm Res 2007, 24, 1–16.

11 Bae, Y.; Nishiyama, N.; Fukushima, S.; Koyama, H.; Yasuhiro, M.; Kataoka, K. Bioconjugate Chem 2005, 16, 122–130.

12 Cabral, H.; Nishiyama, N.; Kataoka, K. J Control Release 2007, 121, 146–155.

13 Du, W.; Nyström, A. M.; Zhang, L.; Powell, K. T.; Li, Y.; Cheng, C.; Wickline, S. A.; Wooley, K. L. Biomacromolecules 2008, 9, 2826–2833.

14 Du, W.; Xu, Z.; Nyström, A. M.; Zhang, K.; Leonard, J. R.; Wooley, K. L. Biomacromolecules 2008, 19, 2492–2498.

15 Chen, Z.; Cui, H.; Hales, K.; Li, Z.; Qi, K.; Pochan, D. J.; Wooley, K. L. J Am Chem Soc 2005, 127, 8592–8593.

16 Hamley, I. W.; Ansari, I. A.; Castelletto, V.; Nuhn, H.; Rosler, A.; Klok, H. A. Biomacromolecules 2005, 6, 1310–1315.

17 Hanley, K. J.; Lodge, T. P.; Huang, C. I. Macromolecules 2000, 33, 5918–5931.

18 Hou, S.; Man, K. Y. K.; Chan, W. K. Langmuir 2003, 19, 2485–2490.

19 Li, Z.; Chen, Z.; Cui, H.; Hales, K.; Qi, K.; Wooley, K. L.; Pochan, D. J. Langmuir 2005, 21, 7533–7539.

20 Zheng, R.; Liu, G.; Yan, X. J Am Chem Soc 2005, 127, 15358–15359.

21 Kubowicz, S.; Baussard, J.-F.; Lutz, J.-F.; Thünemann, A. F.; Berlepsch, H. V.; Laschewsky, A. Angew Chem Int Ed 2005, 44, 5262–5265.

22 Li, Z.; Hillmyer, M. A.; Lodge, T. P. Langmuir 2006, 22, 9409–9417.

23 Lodge, T. P.; Hillmyer, M. A.; Zhou, Z.; Talmon, Y. Macromolecules 2004, 37, 6680–6682.

24 Cui, H.; Chen, Z.; Zhong, S.; Wooley, K. L.; Pochan, D. J. Science 2007, 317, 647–650.

25 Liu, C.; Hillmyer, M. A.; Lodge, T. P. Langmuir 2009, 25, 13718–13725.

26 Saito, N.; Liu, C.; Lodge, T. P.; Hillmyer, M. A. Macromolecules 2008, 41, 8815–8822.

27 Lodge, T. P.; Rasdal, A.; Li, Z.; Hillmyer, M. A. J Am Chem Soc 2005, 127, 17608–17609.

28 Kotzev, A.; Laschewsky, A.; Adriaensens, P.; Gelan, J. Macromolecules 2002, 35, 1091–1101.

29 Stahler, K.; Selb, J.; Candau, F. Langmuir 1999, 15, 7565–7576.

30 Nasongkla, N.; Bey, E.; Ren, J.; Ai, H.; Khemtong, C.; Guthi, J. S.; Chin, S. F.; Sherry, A. D.; Boothman, D. A.; Gao, J. Nano Lett 2006, 6, 2427–2430.

31 Sawant, R. M.; Hurley, J. P.; Salmaso, S.; Kale, A.; Tolcheva, E.; Levchenko, T. S.; Torchilin, V. P. Bioconjugate Chem 2006, 17, 943–949.

32 Solomatin, S. V.; Bronich, T. K.; Eisenberg, A.; Kabanov, V. Z.; Kabanov, A. V. Langmuir 2007, 23, 2838–2842.

33 Cui, H.; Chen, Z.; Wooley, K. L.; Pochan, D. J. Macromolecules 2006, 39, 6599–6607.

34 Kricheldorf, H. R. J Polym Sci Part A: Polym Chem 2009, 47, 1971–1987.

35 Hawker, C. J.; Lee, R.; Fréchet, J. M. J. J Am Chem Soc 2002, 113, 4583–4588.

36 Hawker, C. J.; Fréchet, J. M. J.; Grubbs, R. B.; Dao, J. J Am Chem Soc 1995, 117, 10763–10764.

37 Fréchet, J. M. J.; Henmi, M.; Gitsov, I.; Aoshima, S.; Leduc, M. R.; Grubbs, R. B. Science 1995, 269, 1080–1083.

38 Matyjaszewski, K.; Gaynor, S. G.; Müller, A. H. E. Macromolecules 1997, 30, 7034–7041.

39 Matyjaszewski, K.; Pyun, J.; Gaynor, S. G. Macromol Rapid Commun 1998, 19, 665–670.

40 Georgi, U.; Erber, M.; Stadermann, J.; Abulikemu, M.; Komber, H.; Lederer, A.; Voit, B. J Polym Sci Part A: Polym Chem 2010, 48, 2224–2235.

41 Tsarevsky, N. V.; Huang, J.; Matyjaszewski, K. J Polym Sci Part A: Polym Chem 2009, 47, 6839–6851.

42 Khan, A.; Malkoch, M.; Montague, M. F.; Hawker, C. J. J Polym Sci Part A: Polym Chem 2008, 46, 6238–6254.

43 Powell, K. T.; Cheng, C.; Wooley, K. L. Macromolecules 2007, 40, 4509–4515.

44 Mao, J.; Ni, P.; Mai, Y.; Yan, D. Langmuir 2007, 23, 5127–5134.

45 Mai, Y.; Zhou, Y.; Yan, D. Macromolecules 2005, 38, 8679–8686.

46 Jia, Z.; Zhou, Y.; Yan, D. J Polym Sci Part A: Polym Chem 2005, 43, 6534–6544.

47 Hong, H.; Mai, Y.; Zhou, Y.; Yan, D.; Cui, J. Macromol Rapid Commun 2007, 28, 591–596.

48 Zhou, Y.; Yan, D. Angew Chem Int Ed 2004, 43, 4896–4899.

49 Tian, H.; Chen, X.; Lin, H.; Deng, C.; Zhang, P.; Wei, Y.; Jing, X. Chem Eur J 2006, 12, 4305–4312.

50 Hong, H.; Mai, Y.; Zhou, Y.; Yan, D.; Chen, Y. J Polym Sci Part A: Polym Chem 2008, 46, 668–681.

51 Urbani, C. N.; Lonsdale, D. E.; Bell, C. A.; Whittaker, M. R.; Monteiro, M. J. J Polym Sci Part A: Polym Chem 2008, 46, 1533–1547.

52 Wang, H.-B.; Chen, X.-S.; Pan, C.-Y. J Polym Sci Part A: Polym Chem 2008, 46, 1388–1401.

53 Gudipati, C. S.; Greenlief, C. M.; Johnson, J. A.; Prayongpan, P.; Wooley, K. L. J Polym Sci Part A: Polym Chem 2004, 42, 6193–6208.

54 Brown, G. O.; Bergquist, C.; Ferm, P.; Wooley, K. L. J Am Chem Soc 2005, 127, 11238–11239.

55 Xu, J.; Bohnsack, D. A.; Mackay, M. E.; Wooley, K. L. J Am Chem Soc 2007, 129, 506–507.

56 Powell, K. T.; Cheng, C.; Wooley, K. L.; Singh, A.; Urban, M. W. J Polym Sci Part A: Polym Chem 2006, 44, 4782–4794.

57 Cheng, C.; Wooley, K. L.; Khoshdel, E. J Polym Sci Part A: Polym Chem 2005, 43, 4754–4770.

58 Gaynor, S. G.; Edelman, S.; Matyjaszewski, K. Macromolecules 1996, 29, 1079–1081.

59 Yan, D.; Zhou, Y.; Hou, J. Science 2004, 303, 65–67.

60 Sun, G.; Hagooly, A.; Xu, J.; Nyström, A. M.; Li, Z.; Rossin, R.; Moore, D. A.; Wooley, K. L.; Welch, M. J. Biomacromolecules 2008, 9, 1997–2006.

61 Pressly, E. D.; Rossin, R.; Hagooly, A.; Fukukawa, K.; Messmore, B. W.; Welch, M. J.; Wooley, K. L.; Lamm, M. S.; Hule, R. A.; Pochan, D. J.; Hawker, C. J. Biomacromolecules 2007, 8, 3126–3134.